APPLIED AND ENVIRONMENTAL MICROBIOLOGY, June 2009, p. 3535–3541 Vol. 75, No. 11
0099-2240/09/$08.00+0 doi:10.1128/AEM.02255-08

Phenotypic Diversity of Infectious Red Sea Bream Iridovirus Isolates from Cultured Fish in Japan▽

Hajime Shinmoto,[1] Ken Taniguchi,[2] Takuya Ikawa,[2] Kenji Kawai,[2] and Syun-ichirou Oshima[1]*

Laboratory of Cell Structure and Function, Division of Marine Bioresource Science, Graduate School of Kuroshio Science, Kochi University, Nankoku, Kochi 783-8502, Japan,[1] and Fish Disease Laboratory, Department of Aquaculture, Kochi University, Nankoku, Kochi 783-8502, Japan[2]

Received 1 October 2008/Accepted 27 March 2009

Megalocytivirus **is causing economically serious mass mortality by infecting fish in and around the Pacific region of Asia. The recent emergence of many new iridoviruses has drawn attention to the marked taxonomic variation within this virus family. Most studies of these viruses have not included extensive study of these emergent species. We explored the emergence of red sea bream iridovirus (RSIV) on a fish farm in Japan, and we specifically endeavored to quantify genetic and phenotypic differences between RSIV isolates using in vitro and in vivo methods. The three isolates had identical major capsid protein sequences, and they were closely related to Korean RSIV isolates. In vitro studies revealed that the isolates differed in replication rate, which was determined by real-time quantitative PCR of viral genomes in infected cells and cell culture supernatant, and in cell viability, estimated by the MTT (3-[4,5-dimethylthiazol-2-yl]-2,5-diphenyltetrazolium bromide) assay for infected cells. In vivo studies showed that the isolates exhibit different virulence characteristics: infected red sea bream showed either acute death or subacute death according to infection with different isolates. Significant differences were seen in the antigenicity of isolates by a formalin-inactivated vaccine test. These results revealed that variant characteristics exist in the same phylogenetic location in emergent iridoviruses. We suggest that this strain variation would expand the host range in iridoviral epidemics.**

Iridoviruses are designated as icosahedral cytoplasmic DNA viruses; this group of viruses has different hosts, including fish, amphibians, and insects, causing economic and environmental problems. The family *Iridoviridae* includes five genera: *Iridovirus*, *Chloriridovirus*, *Ranavirus*, *Lymphocystivirus*, and *Megalocytivirus* (45). Piscine iridoviruses belong to the genera *Ranavirus*, *Lymphocystivirus*, and *Megalocytivirus.* In recent years, the genotypical variation between newly found iridovirus strains included in the genus *Ranavirus* has been studied in this viral family (5). However, the properties of and variation between iridovirus species have not been well characterized except for a few iridoviruses isolated from amphibians (11, 46), fish (8, 18, 19), and insects (23, 42, 44). Most studies attempting to differentiate variants have relied on genotypic rather than phenotypic properties.

Members of the *Megalocytivirus* genus produce characteristic basophilic inclusion bodies in the enlarged cells of host fish organs, which have been collected from mass mortalities occurring in wild and cultured fish species (14, 37). Red sea bream (*Pagrus major*) aquaculture has suffered great losses from the prevalence of red sea bream iridovirus (RSIV) infection in Japan. RSIV has been assigned to the *Megalocytivirus* genus. The virus was first isolated from cultured red sea bream in western Japan in 1990 (22).

Many other piscine iridoviruses have been reported in Asian countries (7, 24, 25) from more than 100 different species (41), including freshwater and marine fish (19). RSIV is closely related genetically to viruses isolated from ornamental fish in Southeast Asia, based on nucleotide sequence studies (21, 39). A formalin-inactivated RSIV vaccine has been used in juvenile marine fish against this disease (31, 32).

The incidence of iridovirus infection has been increasing among cultured fish in Japan (29, 30). In addition, genetic and phenotypic iridovirus variants suggest the presence of diverse variants in this virus group (16). In the present study, we examined the detailed properties of three RSIV isolates from two fish species collected from fish farms in western Japan. Using in vitro and in vivo processes, we focused close examination specifically on quantitative genetic and phenotypic differences between the three isolates. The aim of this study was to increase understanding of the epidemiology of RSIV.

MATERIALS AND METHODS

Viruses and cells. Viral isolates from three individual fish specimens (farm cultured) were used in this study. The first isolate (strain U-1) was isolated from an RSIV-infected red sea bream from Uranouchi Bay, Kochi, Japan, in 2001 (20). The second isolate (strain KST-Y-1) was isolated from an RSIV-infected yellow tail in Mitoyo, Kagawa, Japan, in 2004. The third isolate (strain U-6) was isolated from an RSIV-infected red sea bream from Uranouchi Bay, Kochi, Japan, in 2005. The isolates were inoculated at a multiplicity of infection of 1.0 onto confluent monolayers of cloned red sea bream fin (CRF-1) cells in 25-cm^2 tissue culture flasks containing 25 ml of Eagle's minimum essential medium with Hanks' balanced salt solution supplemented with 10% fetal bovine serum, 100 U penicillin/ml, 100 μg/ml streptomycin, and 200 μg/ml neomycin and incubated at 24°C for 5 days or up to the time point at which maximum cytopathic effect was observed (21).

PCR and DNA sequencing. Each viral isolate was inoculated onto confluent monolayers of CRF-1 cells in three replicate 25-cm^2 flasks as described above. DNA extraction from these iridovirus isolates was performed by a proteinase K lysis method (30). Briefly, the infected cell culture including supernatant was centrifuged at 50 × *g* for 20 min at 4°C. Then, the precipitate containing free virus particles and cell-associated nucleocapsids was digested with 100 U/ml

* Corresponding author. Mailing address: Laboratory of Cell structure and Function, Division of Marine Bioresource Science, Graduate School of Kuroshio Science, Kochi University, Nankoku, Kochi 783-8502, Japan. Phone and fax: 81 88 864 5214. E-mail: S-Oshima@cc.kochi-u.ac.jp.

▽ Published ahead of print on 3 April 2009.

TABLE 1. Primers used for PCR-RFLP analysis in this study

Primer set	Region[a]	Primer sequence (5′–3′)
Set 1	1L-6L	TGATCTTTTAATACCCCTG
		GCCACCAACTATGCGTTACG
Set 2	20R-22R	GCCACACTGCGCCACAGTG
		TGTTTGTGCACGTACGCCAAC
Set 3	32L-35L	TCAAATGCGATAGCGCTTGC
		GGCTGTGTATATCAGCTACT
Set 4	45L-50R	CGCGTAACAGGCGCCAGTC
		GTGTCGCCCGCCCACGCGAC
Set 5	71L-73R	GTGCACATGACGGCCGATGAG
		CGGTGAAACACTTGAAGCC
Set 6	85R-88L	ATAAAACTGATTGTGGTGCC
		GACAGCGTTGGCCAGCTGCT
Set 7	111L-112R	GTGTCTCTCAGTCATGATGAC
		CGGGCAACAGGCAGACGCATG

[a] Regions were numbered according to OSGIV open reading frames (GenBank accession number AY894343).

proteinase K at 55°C for 2 h and subjected to phenol-chloroform DNA extraction. The concentrations and purity of the extracted DNA were determined spectrophotometrically.

A specific primer set for major capsid protein (MCP) genes of RSIV was designed from the RSIV ehime-1 strain sequence (GenBank accession number AB080362) and rock sea bream iridovirus (RBIV) sequence (GenBank accession number AY532609) (9). This region was amplified with *Ex Taq* polymerase (Takara Bio Inc.). The thermal cycling conditions consisted of 35 cycles of denaturation for 1 min at 94°C, annealing for 1 min at 54°C, and extension at 72°C, followed by a final extension at 72°C for 5 min. The PCR products were purified with a commercial kit (Easytrap, version 2; Takara Bio Inc.) and cloned into a plasmid vector for subsequent transformation of *Escherichia coli* with a commercial kit (pGEM-T Easy Vector System; Promega Corp.). Plasmid DNA was purified from *E. coli* cells with a commercial kit (QIAprep Miniprep System; Qiagen, Inc.) for sequence analysis using the automated DNA sequencer ABI Prism 3100-Avant Genetic Analyzer (Applied Biosystems).

Phylogenetic analysis. The DNA sequences were compared with the GenBank/EMBL databases using BLAST (National Center for Biotechnology Information). Sequences were aligned using Clustal W (40), and then a phylogenetic tree was made with the TreeView program (33). The phylogenetic relationships between species were determined using the neighbor-joining method (36), and the reliability of the neighbor-joining tree was inferred using the bootstrap method (12) with 1,000 replicates.

PCR-RFLP analysis. In order to detect genetic differences in the three RSIV isolates, restriction fragment length polymorphism (RFLP) analysis was employed. Each viral isolate was inoculated onto confluent monolayers of CRF-1 cells in three replicates of 25-cm^2 flasks as described above. The flasks were frozen and thawed three times. The infected cell cultures including supernatant were centrifuged at 50 × *g* for 20 min at 4°C. The supernatants containing free viral particles and cell-associated nucleocapsids were treated with DNase at 37°C for 30 min and then boiled at 94°C for 30 min. The solutions were digested with proteinase K (0.2 mg/ml) at 55°C for 2 h, subjected to phenol-chloroform extraction, and then precipitated with ethanol.

We designed seven primer sets for the amplification of RSIV genomic DNA and RFLP analysis, as shown in Table 1. These regions were amplified with LA *Taq* polymerase (Takara Bio Inc.) and 50 pmol of each primer. Reaction conditions consisted of an initial denaturation step at 94°C for 1 min, followed by 35 cycles of denaturation (94°C for 30 s), annealing (52 to 60°C for 30 s), and extension (72°C for 2 to 4 min) and a final extension step at 72°C for 7 min. The products were digested with restriction enzymes HaeII, HapII, and NdeI (Takara Bio Inc.), reacted for 6 h. Digested products were separated by 1.2% agarose gel electrophoresis, stained with ethidium bromide, and photographed under UV illumination.

Real-time qPCR. Oligonucleotide sequences were determined by referencing with an orange-spotted grouper iridovirus (OSGIV) structural gene for ATPase (GenBank accession number AY894343) (27). Primer Express software (version 1.5; PE Applied Biosystems) was used to design a TaqMan probe (5′-FAM-AAATCTATCATTGCAGCCAAGCGGC-TAMRA-3′, where FAM is 6-carboxyfluorescein and TAMRA is 6-carboxytetramethylrhodamine) and the forward (5′-GCGGCAAGTCGGTGCTAA-3′) and reverse (5′-CGCGGCGGGA ATTATG-3′) PCR primer set, and the locations were nucleotides 98 to 115 on the forward side, 117 to 142 on the proof side, and 144 to 159 and on the reverse side. The primers and probe, designed to anneal and amplify a 61-bp target sequence within the ATPase gene, were assessed for species specificity by BLAST search to determine homology to known sequences. The quantitative PCR (qPCR) was performed in triplicate for each sample in a 25-μl reaction mixture containing 12.5 μl of 2× TaqMan Universal PCR Master Mix (Applied Biosystems, Inc.), 2.5 μl of template DNA, 900 nmol of each primer, and 250 nmol of fluorescent probe in a 96-well optical PCR plate, which was set on an ABI Prism 7300 Sequence Detection System (Applied Biosystems, Inc.). The real-time PCR protocol consisted of holding samples at 50°C for 2 min, followed by denaturation at 95°C for 10 min and then 40 cycles of 95°C for 15 s and 60°C for 1 min.

The qPCR was standardized by using a DNA sample with serial concentrations. An approximately full-length fragment of the RSIV ATPase gene, containing the full 61-bp target sequence, was a specific primer set for the ATPase of this virus. We designed the forward (5′-ATGGAAATCCAAGAGTTGTCC CTG-3′) and reverse (5′-TTACACCACGCCAGCCTTG-3′) PCR primers. This region was amplified with Ex *Taq* polymerase. The thermal cycling conditions consisted of 35 cycles of denaturation for 1 min at 94°C, annealing for 1 min at 54°C, and extension at 72°C, followed by a final extension for 5 min at 72°C. The amplicon was cloned into a plasmid vector and purified with plasmid DNA as described above. The DNA concentration was determined using a competitive PCR with a commercial kit (Competitive DNA Construction Kit; Takara Bio, Inc.). Serial dilution was used to prepare standards that ranged in concentration from 10^1 to 10^8 copies per μl. qPCR was performed on these standards, as described above, and linear regression was used to create a standard curve for interpolating the concentrations of unknown samples. Variability in the qPCR was measured as the square of Pearson's product-moment correlation coefficient (r^2) describing the relationship between the known concentrations of standards and their concentrations inferred by qPCR.

Analysis of viral replication. Replication profiles of the three RSIV isolates were analyzed in vitro. Confluent monolayers of CRF-1 cells in three replicate 25-cm^2 tissue culture flasks containing 10 ml of medium were prepared as described above. The cells were inoculated with 500 μl of each RSIV isolate containing 10^3 copies of viral DNA solution at a multiplicity of infection of 1.0, with two uninoculated flasks to serve as controls.

Every 24 h, 0.3 ml of cell culture supernatant was removed from each flask, and the infected cells were collected from each flask at each time point. The viral DNA was extracted using a commercial kit (QIAamp DNA Blood Mini Kit; Qiagen, Inc.). Virus concentration (genomes per milliliter) was determined by real-time qPCR for each isolate at each time point.

MTT assay. An MTT (3-[4,5-dimethylthiazol-2-yl]-2,5-diphenyltetrazolium bromide) assay was performed to analyze dead or live virus-infected cells. CRF-1 cell monolayers were prepared in 96-well tissue culture plates where approximately 5×10^4 cells per well were seeded and then cultured overnight at 24°C. An MTT assay was performed on each monolayer after inoculation with 50 μl of a DNA solution containing 10^3 virus copies using a commercial kit (MTT cell count kit; Nakalai Tesque). Briefly, the cultured monolayers were inoculated with RSIV culture supernatant, and then every 24 h MTT was added to each well. After incubation for 4 h at 24°C, culture medium was removed from the well, and then formazan precipitate dissolved in dimethyl sulfoxide was added. The absorbance of the mixture was determined at 570 nm (reference, 670 nm) using Mutiscan JX, version 1.1 (Thermo Lab Systems), in duplicate.

Electron microscopy. Virus particles in infected cultured cells were observed by transmission electron microscopy. CRF-1 cells were infected with U-1, KST-Y-1, or U-6 virus and then fixed at every 24 h in 2.5% glutaraldehyde overnight at 4°C. The cells were sectioned by ultramicrotome and stained with uranyl acetate, and then virus particles were observed using transmission electron microscopy (H-7100; Hitachi).

Experimental challenge and sampling of tissue and organs. Juvenile red sea bream (body weight, 8.29 ± 3.8 g) were used for virulence testing. Three sets of 50 fish each were kept in 200-liter aquaria with running seawater, which was recirculated at a temperature of 28°C. Each set of fish was divided into four groups and challenged intraperitoneally with a different dose of three RSIV isolates or with phosphate-buffered saline (PBS) in control groups. First, one group from each set was inoculated with 10^3 50% tissue culture infective doses (10^3 $TCID_{50}$)/fish of U-1, U-6, and KST-Y-1 virus. The second and third groups from each set received 10^4 and 10^5 $TCID_{50}$/fish, respectively, of the three strains. The fourth group from each set was injected with PBS as a control. Cumulative mortality was examined for 14 days. Tissues were collected from fish infected with a 60% lethal dose: for U-1, 10^4 $TCID_{50}$ /fish; for U-6, 10^3 $TCID_{50}$/fish; and for KST-Y-1, 10^4 $TCID_{50}$/fish. Three to 10 days after infection, six fish were

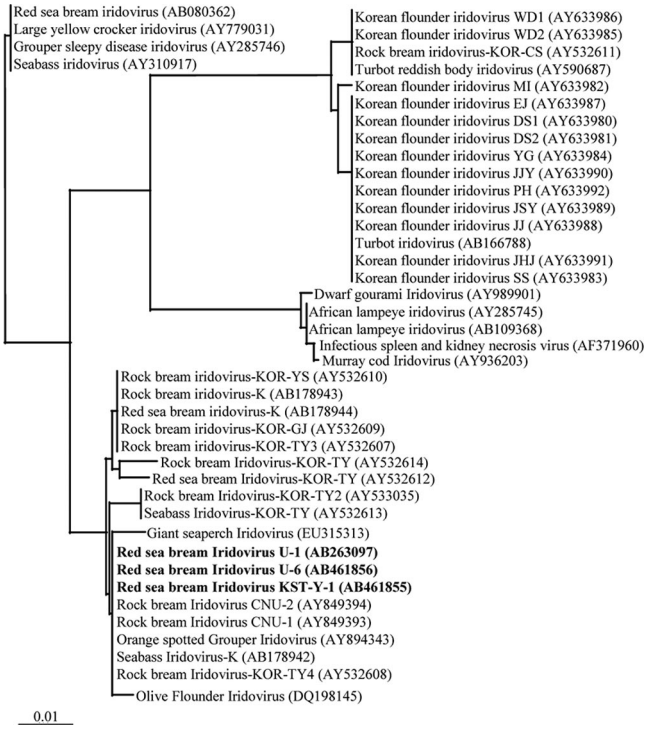

FIG. 1. Phylogenetic analysis of MCP sequences. All sequences were available in the GenBank and were analyzed using the Clustal W program. RSIV strain ehime-1 was used as the outgroup. The significance of branching order was assessed by bootstrap resampling of 1,000 replicates. The RSIV isolate sequenced in this study is represented in boldface. Genetic distance was proportional to horizontal branch length and is indicated at the bottom of the figure.

randomly collected from each group, and tissue samples were harvested from the spleen, kidney, liver, heart, brain, and suborbital musculature. Tissue samples from three fish were stored at −80°C, and those from another three fish were fixed in 3% formalin (Sigma, St. Louis, MO) in PBS for 24 h and stocked in the same fresh formalin solution until pathological observation.

Virus distribution in fish organs. Tissue samples from the infected fish were homogenized in PBS and centrifuged at 2,500 × *g* for 10 min. The supernatant was digested with protease K (0.2 mg/ml) at 55°C for 2 h, followed by phenol-chloroform extraction and ethyl alcohol precipitation. The genomic DNA in the precipitates was dissolved in a Tris-EDTA buffer and used as a template for detecting the RSIV ATPase gene described above. The PCR products were separated by 1.2% agarose gel electrophoresis, stained with ethidium bromide, and photographed under UV illumination.

Pathological observation. Fixed tissue samples were dehydrated in ethanol and embedded in paraffin. The embedded tissues were sectioned about 5 μm thick, stained with hematoxylin and eosin, and then observed under a microscope.

Preparation of vaccine. A formalin-inactivated RSIV vaccine was prepared as described previously (32). Briefly, CRF-1 cells infected with the three strains, U-1, U-6, and KST-Y-1, were collected and centrifuged at 2,500 × *g* for 10 min at 4°C. Formalin (0.3%) was then added to the supernatant, which contained $10^{6.5}$ $TCID_{50}$/ml virus. The virus was inactivated for 10 days at 4°C. Thus, three inactivated vaccines were prepared.

Vaccination and challenge. A total of 1,200 juvenile red sea bream (body weight, 8.3 ± 3.8 g) were used as experimental fish. The fish were divided into two sets of four groups. Each group consisted of 150 fish, which were reared in an 800-liter aquarium supplied with running seawater at a controlled temperature of 28°C. In one set of fish, three groups were intraperitoneally injected with 0.1 ml of each vaccine preparation. The fourth group of fish received a PBS injection as a control. Another set of four groups was immunized similarly. Three weeks after vaccination, all the fish groups were challenged by intraperitoneal infection with 0.1 ml of RSIV (U-6 strain) solution. The challenge test was conducted by intraperitoneal injection with two doses of the RSIV U-6 strain. One set (consisting of four groups) of fish was infected with RSIV at 10^4 $TCID_{50}$/fish, and another set was infected with 10^3 $TCID_{50}$/fish. The fish were observed for 14 days for the clinical signs of disease, and dead fish were collected every day. Statistical analysis was carried out using Fisher's exact test. The relative percentage survival (RPS) (1) was determined by the following formula: RPS = [1− (percent mortality of immunized fish/percent mortality of control fish)] × 100.

Nucleotide sequence accession numbers. The nucleotide sequences of the RSIV MCP region were deposited in the GenBank database under accession numbers AB461856 (U-6) and AB461855 (KST-Y-1).

RESULTS

Phylogenetic analysis. The relationship between isolates and previously reported iridoviruses (2, 9, 10, 15, 17, 21, 25, 27, 37, 39, 43) was determined by phylogenetic analysis (12, 36). There were sequence variations in the MCP regions among the isolates; however, all of the samples were similar to foreign isolates, including OSGIV and RBIV (Fig. 1).

Genetic differences among isolates. PCR-RFLP to detect genetic differences in the three isolates showed different patterns of banding in two of the seven selective regions (Fig. 2). In set 2, the banding pattern of U-6 showed differences from the other two isolates. In the set 4, the banding pattern of U-1 showed differences from the two other isolates. Sets 1, 3, 5, 6, and 7 did not show different banding patterns among the three isolates.

Replication profile and virulence differences in vitro. Viral replication was examined using real-time PCR with viral DNA extracted from RSIV-infected CRF-1 cells and cell culture

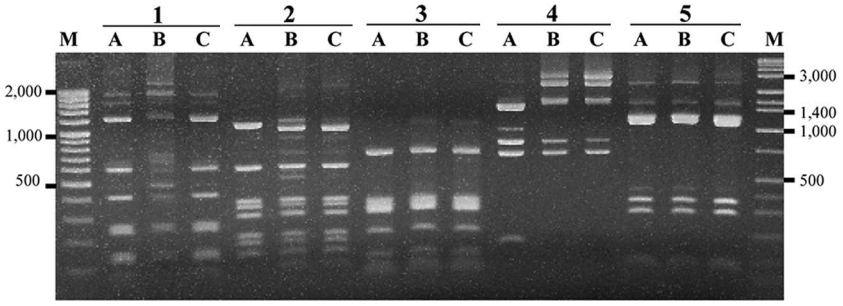

FIG. 2. RFLP analysis of the three RSIV isolates. Lanes M indicate DNA length markers as follows: left, One Step Ladder 100 (Wako); right, All Purpose Hi-Lo (Bionexus, Inc.). The lengths of specific marker bands (base pairs) are indicated at the right and left of the gel. Lanes A, B, and C show RSIV isolates U-1, U-6, and KST-Y-1, respectively. Numbers above the lanes designate the sets of amplified regions and restriction enzymes used as follows: 1, set 2 and HaeII; 2, set 4 and HaeII; 3, set 4 and HapII; 4, set 4 and NdeI; 5, set 6 and HapII.

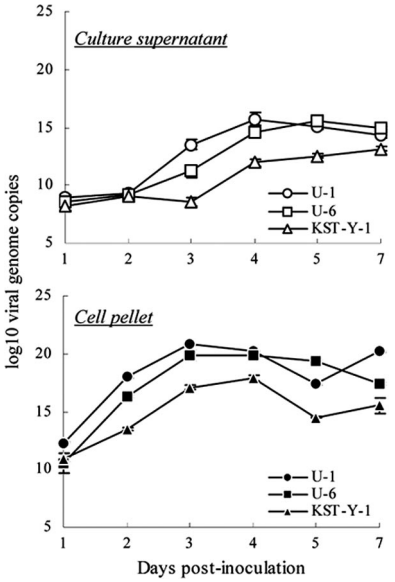

FIG. 3. Viral genome copies in supernatant and cell pellets from CRF-1 cell cultures inoculated with three RSIV isolates determined by real-time qPCR. Points represent mean values of duplicated cell culture flasks inoculated with each isolate.

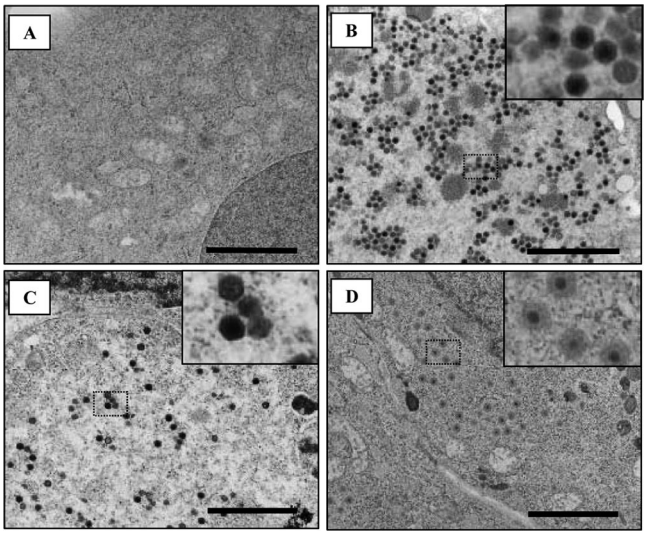

FIG. 5. Transmission electron microscopy images of RSIV particles observed in CRF-1 cells infected with the three RSIV isolates. Images are of mock-infected cells (A) and cells infected with U-1 (B), U-6 (C), or KST-Y-1 (D) virus. Virus particles were observed in small aggregates in the cytoplasm after 48 h in U-1- and U-6-infected cells and after 96 h in KST-Y-1-infected cells. Insets in each panel show magnified images. Bar, 2.0 μm.

supernatant at the times indicated on Fig. 3. The replication profile for KST-Y-1 differed from the profiles for U-1 and U-6. The replication peak for KST-Y-1 appeared around 5 to 7 days postinoculation, whereas the replication peak for U-6 and U-1 appeared at 3 days postinoculation.

An MTT assay was carried out to determine the virulence of the three viral isolates in CRF-1 cells. Cell viability was determined by the relative rate of absorbance of infected cells compared with that of mock-infected cells (Fig. 4). Significant differences in cell viability were observed between cells infected with the three RSIV isolates. The mean viability of cells infected with U-6, KST-Y-1, and U-1 was 52%, 70%, and 4%, respectively. Cells infected with U-1 experienced 33% viability by day 4 postinoculation.

Electron microscopy. Virus particles of the three isolates appeared at different inoculation times in the CRF-1 cell culture. The virus particles of U-1, U-6, and KST-Y-1 isolates appeared at 2, 2, and 4 days after inoculation, respectively (Fig. 5). Virus particles were observed in small aggregations in the cytoplasm of infected cells. Some results were observed in replicates.

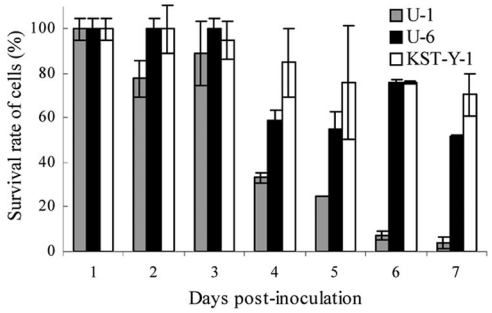

FIG. 4. Survival rate of CRF-1 cells infected with three RSIV isolates measured by MTT assay. Infection dose was 50 μl of 10^3 copies of viral DNA of each isolate. Cell viability was calculated as the relative rate of absorbance in virus-infected cells compared with that in mock-infected cells and is represented as mean ± standard deviation.

Virulence and virus distribution in infected fish. Mortality profiles in fish infected with the three RSIV isolates are shown in Fig. 6. Significant differences were detected between fish infected with doses of 10^5, 10^4, and 10^3 $TCID_{50}$ of the three RSIV isolates, U-1, U-6, and KST-Y-1. Fish infected with U-6 showed a typical acute progression of the disease, and all infected fish died within 7 to 9 days postinfection with 10^5 or 10^4 $TCID_{50}$/fish. In contrast, 100%, 70%, and 30% of fish infected with KST-Y-1 at 10^5, 10^4, and 10^3 $TCID_{50}$/fish, respectively, died within 8 to 11 days. Fish infected with U-1 at 10^5, 10^4, and 10^3 $TCID_{50}$/fish showed 70%, 60%, and 20% mortality, respectively, within 7 to 10 days. No morbidity or mortality was observed in PBS-injected control fish.

Viral DNA was detected in all the selected tissues (liver, kidney, spleen, heart, brain, and suborbital musculature) of fish from 5 to 10 days after infection (Fig. 7). The spleen, liver, and kidney tissues showed relatively strong signals. The DNA of the U-6 strain had a different profile from the U-1 and KST-Y-1 strains and was detected in all tissues within 5 to 8 days postinjection. The DNA of the KST-Y-1 strain was first observed in four tissues, spleen, kidney, liver, and heart, after which it appeared in the brain and suborbital musculature. Control fish were negative for viral DNA in all tissues throughout the experimental period.

Enlarged cells were observed in the spleen, kidney, and liver of three juvenile red sea bream 5 to 10 days after injection with the three RSIV strains, and the spleen showed the highest number of such cells.

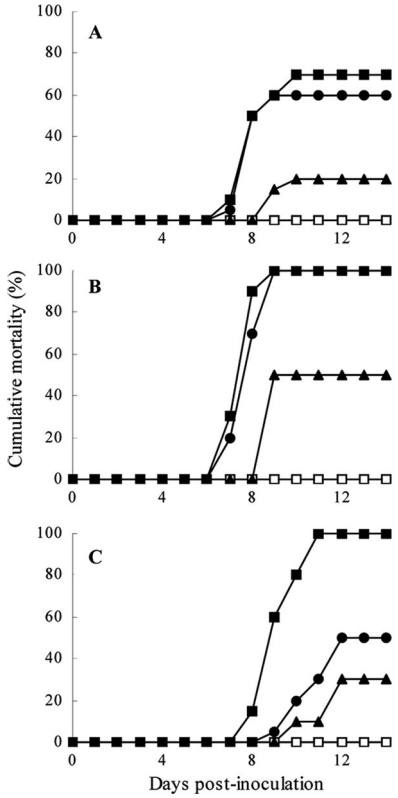

FIG. 6. Cumulative mortality of red sea bream infected intraperitoneally with three doses of the RSIV isolates U-1 (A), U-6 (B), and KST-Y-1 (C). Infection doses are as follows: 10^5 (■), 10^4 (●), and 10^3 (▲) $TCID_{50}$/fish, and PBS as a control (□). RSIV was not detected in mock-infected control fish.

Mortality after challenge of immunized fish. Figure 8 shows differences in the protective effects of vaccination in the immunized groups at two infection doses. Fish that were vaccinated with the vaccine for the U-6 strain showed the highest survival rate, whereas fish vaccinated with the vaccine for the KST-Y-1 strain showed the lowest survival rate. RPS values obtained for the fish immunized with U-6, U-1, and KST-Y-1 strains were 69, 45, and 11%, respectively, at the higher infection dose.

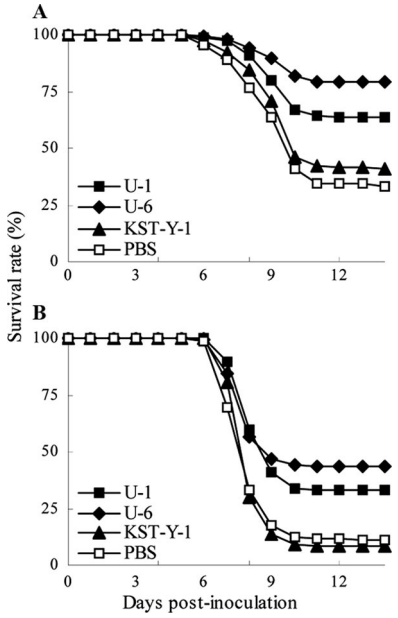

FIG. 8. Survival rate of vaccinated fish after challenge with at a high dose and low dose of the U-6 strain. Infection doses were 10^3 $TCID_{50}$/fish (A) and 10^4 $TCID_{50}$/fish (B).

DISCUSSION

Megalocytiviruses have been isolated from different fish species and are considered pathogens of diseases that cause significant economic losses in the fish aquaculture industry (2, 6, 7, 25, 31, 37, 38, 39). Most studies of these viruses have been on the genetic relationships between emerging strains; however, studies linking these genetic findings to viral phenotypic characteristics are almost absent. One objective of this study was to clarify the phenotypes, especially virulence characteristics, of different emerging viral isolates.

We have demonstrated that RSIVs isolated from western Japan differ genetically and pathogenically in vivo and in vitro. Nucleotide sequence and phylogenetic analysis revealed that most of the isolates were similar to OSGIV, RBIV, and grouper sleepy disease virus, demonstrating that RSIV isolates have different phenotypes. The three isolates showed different band patterns by RFLP analysis.

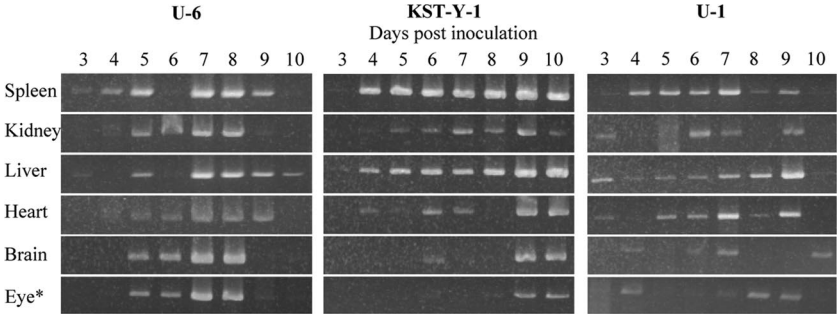

FIG. 7. Distribution of the RSIV ATPase gene in the tissue of red sea bream infected with the three RSIV isolates at a 60% lethal dose: for U-1, 10^4 $TCID_{50}$/fish; for U-6, 10^3 $TCID_{50}$/fish; and for KST-Y-1, 10^4 $TCID_{50}$/fish. Virus was detected by PCR. Eye* indicates eye musculature tissue.

Phenotypical differences were also observed among the three isolates in vitro. U-6 and U-1 showed higher replication rates and virulence than KST-Y-1 in CRF-1 cells that originated from the fin tissue of red sea bream. Virus particles appeared in U-6- and U-1-infected cells earlier than in KST-Y-1-infected cells. Higher viral replication and virulence were found in the red sea bream isolates U-1 and U-6, whereas the KST-Y-1 yellow tail isolates showed low activity.

The isolates also showed different virulence profiles in an experimental infection in juvenile red sea bream. U-6 was highly virulent, showing acute progression and death, whereas KST-Y-1 and U-1 demonstrated subacute profiles. To assess viral tropism, virus distribution in fish tissues after RSIV infection was examined, and differences in the proliferation and distribution of virus strains were observed. U-6 had broad distribution in the heart, brain, and eye musculature. Numerous accumulations of KST-Y-1 virus particles were found in the spleen, liver, and kidney, and distribution in the heart, brain, and eye musculature occurred in the late stages of infection. U-1 showed numerous accumulations of virus in the spleen and liver; however, this strain also had broad distribution with slight detection in other tissues. These results show that the variation in distribution for these different emerging viral isolates is strongly related to their virulence profiles.

In *Megalocytivirus* infection, diseased fish show numerous accumulations of virus particles in the spleen and kidney (6, 39). The spleen has been reported to be the most susceptible organ in iridoviral disease (28). The three isolates used in the infection experiment showed the accumulation of virus genes in the spleen and kidney; however, virus genes were detected in the liver, heart, brain, and eye musculature at the time many fish were dying. These results suggest that systemic proliferation of the virus readily causes the death of fish. A similar disease profile has been reported for the frog virus 3, a virus of the *Ranavirus* genus. A susceptible amphibian species infected with the virus showed preferential distribution of the virus in the kidney although the animal persisted for a long time (13); however, systemic spreading of the virus to most organs in the visceral cavity caused acute disease progression and death (35). The virulence mechanisms of megalocytiviruses have been studied in vitro; however, very few attempts have been made to characterize strain-specific virulence factors as well as to elucidate host-related and ecological factors in vivo.

The three isolates used in this study have the same MCP nucleotide sequence; however, different levels of protection occurred in the immunization and challenge experiments. Immunization with U-6 was significantly protective against U-6-infection in juvenile red sea bream, showing a more than 35% higher protection rate than KST-Y-1 immunization and more than 10% higher protection than U-1 immunization. Previous studies suggest that the MCP gene of RSIV is an effective component in a genetic vaccine test (4, 26) and a formalin-inactivated virus vaccine test (3). The formalin-inactivated virus vaccine used in this study represents the MCP region plus other gene products of the virus. These results suggest that careful selection of viral strains is necessary when inactivated vaccine is being developed.

It has been suggested that the worldwide distributed megalocytiviruses have a common origin (38, 39). Furthermore, it has been strongly suggested that iridoviruses and recently discovered viruses lately differentiated from the same origin (15). The present study has revealed that iridoviruses include variants although they are located in the same phylogenetic position according to the MCP gene sequence. Additionally, the result of this study revealed that viruses with different phenotypes infect the same species of host. Similar cases were reported also for largemouth bass virus (16). Our results support a hypothesis that there are many phenotypes of viruses of the *Iridoviridae* family in the environment and that these viruses infect different host species, cause different symptoms, and produce different mortality rates. In order to elucidate this presumption, further study is necessary. In *Iridoviridae*, there is a lack of information about genome organization or factors affecting host range. The aim of our work is to find effective ways of controlling the iridovirus infection, and we hope the findings in this study will be useful.

ACKNOWLEDGMENTS

We thank T. Taniguchi and K. Yagyu, Kochi Medical School, for their sincere technical advice.

This research was supported by a Research for Promoting Technological Seeds grant from the Japan Science and Technology Agency (JST).

REFERENCES

1. **Amend, D.** 1981. Potency testing of fish vaccines. Dev. Biol. Stand. **49:**447–454.
2. **Ao, J., and X. Chen.** 2006. Identification and characterization of a novel gene encoding an RGD-containing protein in large yellow croaker iridovirus. Virology **355:**213–222.
3. **Caipang, C. M. A., T. Takano, I. Hirono, and T. Aoki.** 2006. Immunogenicity, retention and protective effects of the protein derivatives of formalin-inactivated red seabream iridovirus (RSIV) vaccine in red sea seabream, *Pagrus major*. Fish Shellfish Immunol. **20:**597–609.
4. **Caipang, C. M. A., T. Takano, I. Hirono, and T. Aoki.** 2006. Genetic vaccines protect red seabream, *Pagrus major*, upon challenge with red seabream iridovirus (RSIV). Fish Shellfish Immunol. **21:**130–138.
5. **Chinchar, V. G.** 2002. Ranaviruses (family *Iridoviridae*): emerging cold-blooded killers. Arch. Virol. **147:**447–470.
6. **Chou, H. Y., C. C. Hsu, and T. Y. Peng.** 1998. Isolation and characterization of a pathogenic iridovirus from cultured grouper (*Epinephelus* sp.) in Taiwan. Fish Pathol. **33:**201–206.
7. **Chua, H. Y., M. L. Ng, J. J. Woo, and J. Y. Wee.** 1994. Investigation of outbreak of a novel disease "Sleepy Grouper Disease" affecting the brown-spotted grouper *Epinephelus tauvina* Forskal. J. Fish Dis. **17:**417–427.
8. **Darai, G., K. Anders, H. G. Koch, H. Delius, H. Gelderblom, C. Samalecos, and R. M. Flugel.** 1983. Analysis of the genome of fish lymphocystis disease virus isolated directly from epidermal tumours of Pleuronectes. Virology **126:**466–479.
9. **Do, J. W., S. J. Cha, J. S. Kim, E. J. An, M. S. Park, J. W. Kim, Y. C. Kim, M. A. Park, and J. W. Park.** 2005. Sequence variation in the gene encoding the major capsid protein of Korean fish iridoviruses. Arch. Virol. **150:**351–359.
10. **Do, J. W., S. J. Cha, J. S. Kim, E. J. An, N. S. Lee, H. J. Choi, C. H. Lee, M. S. Park, J. W. Kim, Y. C. Kim, and J. W. Park.** 2005. Phylogenetic analysis of the major capsid protein gene of iridovirus isolates from cultured flounders Paralichthys olivaceus in Korea. Dis. Aquat. Organ. **64:**193–200.
11. **Essani, K., and A. Granoff.** 1989. Amphibian and piscine iridoviruses: proposal for nomenclature and taxonomy based on molecular and biological properties. Intervirology **30:**187–193.
12. **Fersentein, J.** 1985. Confidence limit on phylogenies: an approach using bootstrap. Evolution **39:**783–791.
13. **Gantress, J., G. D. Maniero, N. Cohen, and J. Robert.** 2003. Development and characterization of a model system to study amphibian immune responses to iridoviruses. Virology **311:**254–262.
14. **Gibson-Kueh, S., P. Netto, G. H. Ngoh-Lim, S. F. Chang, L. L. Ho, Q. W. Qin, F. H. C. Chua, M. L. Ng, and H. W. Ferguson.** 2003. The pathology of systemic iridoviral disease in fish. J. Comp. Pathol. **129:**111–119.
15. **Go, J., M. Lancaster, K. Deece, O. Dhungyel, and R. Whittington.** 2006. The molecular epidemiology of iridovirus in Murray cod (Maccullochella peelii peelii) and dwarf gourami (Colisa lalia) from distant biogeographical regions suggests a link between trade in ornamental fish and emerging iridoviral diseases. Mol. Cell. Probes **20:**212–222.
16. **Goldberg, T. L., D. A. Coleman, E. C. Grant, K. R. Inendino, and D. P.**

Philipp. 2003. Strain variation in an emerging iridovirus of warm-water fishes. J. Virol. **77:**8812–8818.
17. **He, J. G., M. Deng, S. P. Weng, Z. Li, S. Y. Zhou, Q. X. Long, X. Z. Wang, and S. M. Chan.** 2001. Complete genome analysis of the mandarin fish infectious spleen and kidney necrosis iridovirus. Virology **291:**126–139.
18. **Hedrick, R. P., T. S. McDowell, W. Ahne, C. Torhy, and P. de Kinkelin.** 1992. Properties of three iridovirus-like agents associated with systemic infections in fish. Dis. Aquat. Organ. **13:**203–209.
19. **Hyatt, A. D., A. R. Gould, Z. Zupanovic, A. A. Cunningham, S. Hengstberger, R. J. Whittington, J. Kattenbelt, and B. E. Coupar.** 2000. Comparative studies of piscine and amphibian iridoviruses. Arch. Virol. **145:**301–331.
20. **Imajoh, M., H. Sugiura, and S. Oshima.** 2004. Morphological changes contribute to apoptotic cell death and are affected by capsase-3 and caspase-6 inhibitors during red sea bream iridovirus permissive replication. Virology **322:**220–230.
21. **Imajoh, M., T. Ikawa, and S. Oshima.** 2007. Characterization of a new fibroblast cell line from a tail fin of red sea bream, Pagrus major, and phylogenetic relationships of a recent RSIV isolate in Japan. Virus Res. **126:**45–52.
22. **Inouye, K., K. Yamano, K. Nakajima, M. Matsuoko, Y. Wada, and M. Sorimachi.** 1992. Iridovirus infection of cultured red sea bream, *Pagrus major*. Fish Pathol. **27:**19–27.
23. **Jakob, N. J., R. G. Kleespies, C. A. Tidona, K. Muller, H. R. Gelderblom, and G. Darai.** 2002. Comparative analysis of the genome and host range characteristics of two insect iridoviruses: Chilo iridescent virus and a cricket iridovirus isolate. J. Gen. Virol. **83:**463–470.
24. **Jeong, J. B., L. J. Jun, M. H. Yoo, M. S. Kim, J. L. Komisar, and H. D. Jeong.** 2003. Characterization of the DNA nucleotide sequences in the genome of red sea bream iridoviruses isolated in Korea. Aquaculture **220:**119–133.
25. **Jung, S. J., and M. J. Oh.** 2000. Iridovirus-like infection associated with high mortalities of striped beakperch, *Oplegnathus fasciatus* (Temminck et Schlegel), in southern coastal areas of the Korean peninsula. J. Fish Dis. **23:**223–226.
26. **Kim, T. J., T. S. Jung, and J. I. Lee.** 2007. Expression and serological application of a capsid protein of an iridovirus isolated from rock bream, *Oplegnathus fasciatus* (Temminck & Schlegel). J. Fish Dis. **30:**691–699.
27. **Lu, L., S. Y. Zhou, C. Chen, S. P. Weng, S.-M. Chan, and J. G. He.** 2005. Complete genome sequence analysis of an iridovirus isolated from the orange-spotted grouper, *Epinephelus coioides*. Virology **339:**81–100.
28. **Lua, D. T., M. Yasuike, I. Hirono, H. Kondo, and T. Aoki.** 2007. Transcriptional profile of red seabream iridovirus in a fish model as revealed by viral DNA microarrays. Virus Gene **35:**449–461.
29. **Matsuoka, S., K. Inouye, and K. Nakajima.** 1996. Cultured fish species affected by red sea bream iridoviral disease from 1991 to 1995. Fish Pathol. **31:**233–234.
30. **Miyata, M., K. Matuno, S. J. Jung, Y. Danayadol, and T. Miyazaki.** 1997. Genetic similarity of iridoviruses from Japan and Thailand. J. Fish Dis. **20:**127–134.
31. **Nakajima, K., and M. Sorimachi.** 1995. Production of monoclonal antibodies against red sea bream iridovirus. Fish Pathol. **30:**47–52.
32. **Nakajima, K., Y. Maeno, J. Kurita, and Y. Inui.** 1997. Vaccination against red sea bream iridoviral disease in red sea bream. Fish Pathol. **32:**205–209.
33. **Nakajima, K., Y. Maeno, A. Honda, K. Yokoyama, T. Tooriyama, and S. Manabe.** 1999. Effectiveness of a vaccine against red sea bream iridoviral disease in a field trial test. Dis. Aquat. Organ. **36:**73–75.
34. **Page, R. D. M.** 1996. TreeView: an application to display phylogenetic tree on personal computer. Comput. Appl. Biosci. **12:**357–358.
35. **Robert, J., H. Morales, W. Buck, N. Cohen, S. Marr, and J. Gantress.** 2005. Adaptive immunity and histopathology in frog virus 3-infected *Xenopus*. Virology **332:**667–675.
36. **Saitou, N., and M. Nei.** 1987. The neighbor-joining method: a new method for reconstructing phylogenetic tree. Mol. Biol. Evol. **4:**406–425.
37. **Shi, C. Y., Y. G. Wang, S. L. Yang, J. Huang, and Q. Y. Wang.** 2004. The first report of an iridovirus-like agent infection in farmed turbot *Scophthalmus maximus* in China. Aquaculture **236:**11–25.
38. **Sudthongkong, C., M. Miyata, and T. Miyazaki.** 2002. Iridovirus disease in two ornamental tropical freshwater fishes: African lampeye and dwarf gourami. Dis. Aquat. Organ. **48:**163–173.
39. **Sudthongkong, C., M. Miyata, and T. Miyazaki.** 2002. Viral DNA sequences of genes encoding the ATPase and the major capsid protein of tropical iridovirus isolates which are pathogenic to fishes in Japan, South China Sea and Southeast Asian countries. Arch. Virol. **147:**2089–2109.
40. **Thompson, J. D., D. G Higgins, and T. J. Gibson.** 1994. CLUSTAL: improving the sensitivity of progressive multiple sequence alignment through sequence weighing, position specific gap penalties and matrix choice. Nucleic Acids Res. **22:**4673–4680.
41. **Tidona, C. A., and G. Darai.** 1997. The complete DNA sequence of lymphocystis disease virus. Virology **230:**207–216.
42. **Webby, R., and J. Kalmakoff.** 1998. Sequence comparison of the major capsid protein gene from 18 diverse iridoviruses. Arch. Virol. **143:**1949–1966.
43. **Wen, C. M., C. W. Lee, C. S. Wang, Y. H. Cheng, and H. Y. Huang.** 2008. Development of two cell lines from *Epinephelus coioides* brain tissue for characterization of betanodavirus and megalocytivirus infectivity and propagation. Aquaculture **278:**14–21.
44. **Williams, T., and J. Cory.** 1993. DNA restriction fragment polymorphism in iridovirus isolates from individual blackflies (Diptera: Simuliidae). Med. Vet. Entomol. **7:**199–201.
45. **Williams, T., V. Barbosa-Solomieu, and V. G. Chinchar.** 2005. A decade of advances in iridovirus research. Adv. Virus Res. **65:**173–248.
46. **Zhang, Q. Y., F. Xiao, Z. Q. Li, J. F. Gui, J. Mao, and V. G. Chinchar.** 2001. Characterization of an iridovirus from the cultured pig frog Rana grylio with lethal syndrome. Dis. Aquat. Organ. **48:**27–36.